16th European Signal Processing Conference (EUSIPCO 2008), Lausanne, Switzerland, August 25-29, 2008, copyright by EURASIP

CHARACTERIZATION AND CALIBRATION OF MEMS INERTIAL MEASUREMENT UNITS

Gökçen Aslan[1,2], Afşar Saranlı[2]

[1]Defence Research and Development Institute (SAGE), TÜBİTAK

[2]Dept. of Electrical and Electronics Eng., Middle East Technical University

gokcen.aslan@tubitak.gov.tr, afsars@metu.edu.tr

ABSTRACT

Widening applications of inertial sensors has triggered the search for cost effective sensors and those based on MEMS technology has been gaining popularity in particular for the lower cost applications. However, inertial sensors are subject to various error sources and characteristics of these should be modelled carefully and corrective calibration performed if these sensors are to be successfully used for body state estimation and navigation. In the present paper, we review noise and deterministic error models of these sensors and consider several static and dynamic inertial sensor calibration tests. We carry out these tests to analyse the errors, derive calibration parameters and review resulting state measurement performance of a particular MEMS inertial sensor (MicroStrain 3DM-GX1) which is popularly available at reasonable cost. We present our results with the associated discussion on sensor performance.

1. INTRODUCTION

Recently, with the availability and reduced cost of Micro Electro-Mechanical Systems (MEMS) technology, inertial sensors find wide application areas, now also in non-military applications. They are particularly essential in the control and navigation of mobile systems. By means of inertial sensor measurements, it is possible to obtain valuable estimates of the body state (e.g. Euler angles, linear and angular velocity, global position) of a mobile robot, a land vehicle, an airplane, a ship or a person. Three orthogonal accelerometers and three orthogonal gyroscopes are combined together to form an inertial measurement unit (IMU) to provide a complete measurement set-up. IMUs are considered as reliable sensors in the sense that their measured physical quantities are associated with planetary physics and cannot be effected artificially from the outside. However these measurements (e.g. rate of turn) need to be integrated to be useful and inherent sensor measurement errors accumulate through the calculation of the output variables of interest (e.g. body attitude). Sensors are produced with different manufacturing techniques resulting in several performance characteristics and prices[3]. MEMS technology offer cost effective solutions for performing inertial measurements although with reduced specifications. In the present paper, the important task of characterization of MEMS IMUs is investigated by working on a particular sensor: The MicroStrain 3DX-GX1.

2. ERROR SOURCES AND MODELS FOR IMUS

Both accelerometers and gyroscopes suffer from measurement errors. *Fixed bias error* is the sensor output observed even in the absence of an applied physical input. This is called *drift* or *g-independent bias* for gyroscopes[1]. *Scale factor error* is the ratio of output change to the input change causing that output. *Cross-coupling errors* are caused by misalignments between the axes of sensor triads which should ideally be placed as an orthogonal triple. In addition, gyroscopes experience *g-dependent bias errors* which are proportional to the applied acceleration.

These errors are represented by a mathematical model. It is critical to know the behaviour of a sensor to make meaningful use of the sensor measurements. The error model is utilized in navigation algorithms to obtain velocity, position and Euler angles which are sometimes called the *navigation outputs*. Eqs. 1 and 2 represent the error models for the accelerometer and the gyroscope triads where $\boldsymbol{\delta f}$ and $\boldsymbol{\delta\omega}$ represent the accelerometer and gyroscope measurement errors respectively.

$$\begin{bmatrix} \delta f_x \\ \delta f_y \\ \delta f_z \end{bmatrix} = B_A + S_A \begin{bmatrix} \alpha_x \\ \alpha_y \\ \alpha_z \end{bmatrix} + M_A \begin{bmatrix} \alpha_x \\ \alpha_y \\ \alpha_z \end{bmatrix} + w_A \tag{1}$$

$$\begin{bmatrix} \delta\omega_x \\ \delta\omega_y \\ \delta\omega_z \end{bmatrix} = B_G + B_g \begin{bmatrix} \alpha_x \\ \alpha_y \\ \alpha_z \end{bmatrix} + S_G \begin{bmatrix} \omega_x \\ \omega_y \\ \omega_z \end{bmatrix} + M_G \begin{bmatrix} \omega_x \\ \omega_y \\ \omega_z \end{bmatrix} + w_G \tag{2}$$

Here, $\boldsymbol{\alpha_x, \alpha_y, \alpha_z}$ are the actual accelerations and $\boldsymbol{\omega_x, \omega_y, \omega_z}$ are the actual angular rates that are applied on each axis. $\mathbf{B_A}$ and $\mathbf{B_G}$ are 3x1 vectors consisting of the bias elements on each axis. $\mathbf{S_A}$ and $\mathbf{S_G}$ are diagonal 3x3 matrices, elements representing the scale factor for each axis. They may be scalar terms if all axes have identical scale factors. $\mathbf{M_A}$ and $\mathbf{M_G}$ are the orthogonality matrices composed of cross coupling error coefficients. Matrix $\mathbf{B_g}$ contains the g-dependent bias coefficients for the gyros. Finally, $\boldsymbol{w_A}$ and $\boldsymbol{w_G}$ are the noise terms which are usually assumed white Gaussian[6].

The general error models given above are also valid for the considered MEMS IMU. Indeed, $\mathbf{M_A}$ and $\mathbf{M_G}$ matrices play a more important role since the raw measurements do not represent an orthogonal right handed coordinate system. To obtain such measurements, the raw data should be multiplied

with these matrices. (The sensor offers to perform this step internally if configured).

3. ERROR ANALYSIS AND SENSOR CHARACTERIZATION

The 3DM-GX1 sensor package is characterized in this work by means of several tests. The sensor contains 3 MEMS accelerometers, 3 MEMS gyroscopes and 3 magnetometers. Communication is via RS232 serial port. The package contains an internal microprocessor running integration algorithms to supply "stabilized" Euler angles to the user if requested. However, any non-trivial applications of these sensors require the algorithm developer to have complete knowledge of these processing steps. In the present work we use the raw sensor outputs and perform all necessary computations externally.

Static, quasi-static and dynamic experiments are conducted for the characterization of the 3DM-GX1. During static tests, data is collected while the sensor is at rest at various configurations. The aim is to calculate calibration parameters. Dynamical tests aim to observe the accuracy of calculated variables under controlled motion scenarios. The procedures and results of these tests are given separately for accelerometers and gyroscopes in the following sections.

3.1 Accelerometer Static Tests

3.1.1 Single Position Static Tests

Data from stationary accelerometers are collected for several hours to observe the mean and standard deviation of the noisy outputs. Ideally, due to the gravitational acceleration, constant outputs are to be observed on all axes. In practice, a noisy characteristic is observed as expected. *Bias stability* is an important issue in calibration and performance classification of accelerometers. Allan-variance tests[4] are carried out to see the change of bias value with time. For the considered sensor, a bias stability of 130μg, 100μg and 43μg are obtained for orthogonalized x, y and z axes respectively.

3.1.2 Multi-Position Static Tests

Multi-position static tests are done with the purpose of determining the static bias, scale factor and scale factor nonlinearity. Accelerometers are mounted on an index table (Figure 1) capable of measurable (manual) axis rotation with a resolution of 1 degree. The table is rotated so that the measured gravitational acceleration is known due to a known angle with the vertical and will vary between 1g and -1g. Two controlled rotary axes of the table apply this gravitational acceleration variation to the y-axis and z-axis of the sensor respectively. Hence, we can measure the decomposition of the gravitational acceleration vector along the corresponding sensor measurement axes. The step size for the test is determined to be 30º resulting in 12 measurement positions for a 360 degree full turn. One minute data is recorded for each step to compensate for noise. We observe a sinusoidal pattern as expected due to the trigonometric functions involved in this decomposition.

Raw sensor outputs collected from raw "Channels" 1 and 2 of 3DM-GX1 are given in Figure 2. Note that raw channels are not necessarily orthogonal to each other. However Ch1, 2 and 3 mostly correspond to the z, y and x-axis respectively after the sensor axis orthogonalization.

Raw sensor output (Figure 2) is compared with sensor input and scaled to physical units after calculating bias and scale factor values. Bias values of Ch. 1 and 2 are obtained as 32846.3 and 32627.7 respectively which match exactly with the manufacturer specification sheet.

Figure 1- Index table with 3DM-GX1 shown on top (330 degrees orientation around the sensor y-axis)

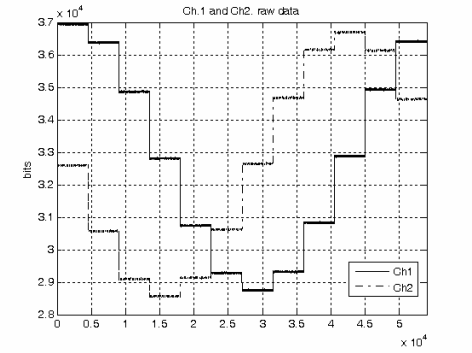

Figure 2- Ch. 1 and Ch. 2 raw outputs

The input and the calibrated output of the sensor for Ch.1 are shown in Figure 3 below. The mean values of 12 data sets are computed and compared with inputs at 12 different positions.

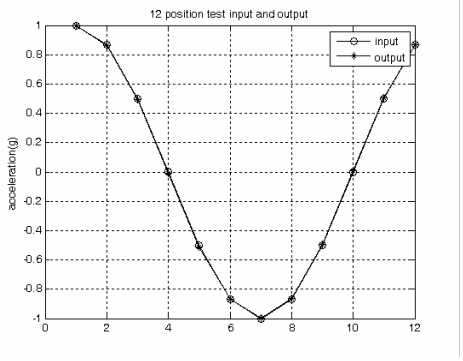

Figure 3- Ch.1 input and calibrated output relationship.

3.1.3 Thermal Test

The performance of MEMS sensors with changing temperature has been studied and it is claimed that a warm-up period is needed for the output to stabilize[2]. In standard IMU cali-

bration, thermal tests are carried out in thermal chambers with carefully controlled internal temperature. Since we did not have this capability, a warm-up test in ambient temperature (25ºC) is conducted. The internal temperature of 3DM-GX1 is observed for 6 hours including its warm-up period where sensor internal temperature increases from ambient to operating value (Figure 4). Data from accelerometers and internal thermometer is collected. Contrary to the observation in [1], no change is observed in output mean values for this sensor (Figure 5). Although not specified by the manufacturer, there may be a temperature compensation algorithm within the sensor processor. Therefore, a thermal error model within this range of temperatures (22ºC to 38ºC) is not recommended. Note however that the there may still be a temperature dependence when the sensor is subjected to higher temperatures.

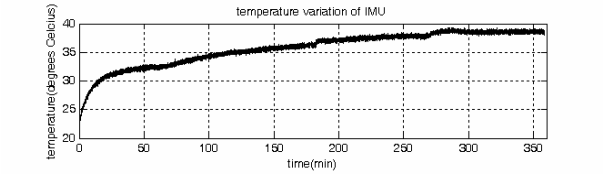

Figure 4- Internal temperature profile (ºC) for 6 hours of MicroStrain 3DM-GX1.

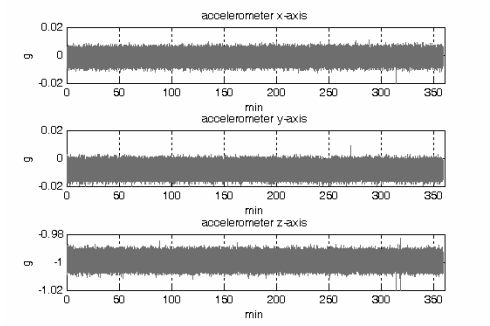

Figure 5- Accelerometer thermal test data. Outputs are recorded for 6 hours.

3.2 Gyroscope Static Tests

3.2.1 Single Position Static Test

3DM-GX1 is capable of supplying accelerometer and gyroscope data concurrently. During the single position static tests described previously, outputs of all sensors are captured. The noise mean and standard deviation for the gyroscope measurements are also examined.

3.2.2 Multi-Position Static Tests

Similar to accelerometer 12 position tests, 8 position tests are carried out for gyroscopes. Through this test, it is possible to collect calibration data about *gyroscopic drift*, *in-run stability*, *g-dependent bias* of the gyroscopes by comparing the input with sensor output[1]. Sensor axes are configured as in Table 1 and the inputs to axes are Earth's rotation rate **Ω** decomposed into components depending on local latitude angle.

position	direction of axes			accelerations on axes			component of Earth's rotation along axes	
	spin	input1	input2	spin	input1	input2	input1	input2
1	up	north	west	1	0	0	ΩcosL	0
2	up	west	south	1	0	0	0	- ΩcosL
3	up	south	east	1	0	0	-ΩcosL	0
4	up	east	north	1	0	0	0	ΩcosL
5	north	east	down	0	0	-1	0	- ΩsinL
6	north	up	east	0	1	0	ΩsinL	0
7	north	west	up	0	0	1	0	ΩsinL
8	north	down	west	0	-1	0	-ΩsinL	0

Table 1- Gyroscope axes configuration for multi-position static tests. Ω stands for Earth's rotation rate which is 15.041°/hour and L stands for the local latitude angle.

The error model for gyroscopes was given in Section 2. For a single axis gyroscope at rest, the error equation can be simplified by eliminating $\mathbf{S_G}$ and $\mathbf{M_G}$ terms since $\boldsymbol{\omega}$ is zero (Eq. 3). It is possible to obtain the values of g-independent and g-dependent bias values for each axis.

$$\delta\omega_x = B_G + B_{gx}a_x + B_{gy}a_y + B_{gz}a_z \tag{3}$$

To find the parameters of x-axis, IMU is placed so that x axis is coincident with the vertical. **+g** and **–g** act to the x-axis when it is placed up and down respectively. The acceleration input on y and z axes are zero. These two measurements are used to calculate $\mathbf{B_G}$ and $\mathbf{B_{gx}}$ (Eq.4). The same procedure can be applied to the other axes to obtain $\mathbf{B_{gy}}$ and $\mathbf{B_{gz}}$.

$$\begin{aligned} m_{x-up} &= B_G + B_{gx}g \\ m_{x-down} &= B_G - B_{gx}g \end{aligned} \tag{4}$$

3.2.3 Thermal Tests

Gyroscope measurements are collected for 6 hours as in the case of accelerometers. Temperature dependence has not been observed in the output data (Figure 6). Therefore, a thermal error model within this range of temperatures (22ºC to 38ºC) is not recommended.

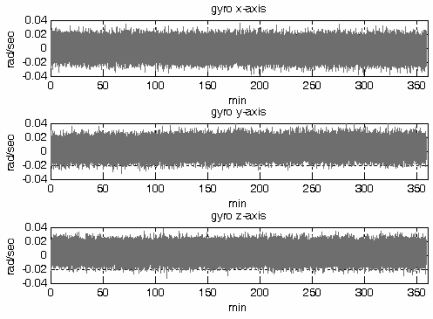

Figure 6 – Gyroscope thermal test data. Outputs are recorded for 6 hours.

3.2.3 Rate Transfer Tests

The purpose of rate transfer tests is to analyse the characteristics of the scale factor, i.e., to analyse the relationship between the change in the input turn rate and the sensor output data as a controlled stepping motion is applied to the sensor. This is realized on a rotating table called *the rate table* [7].

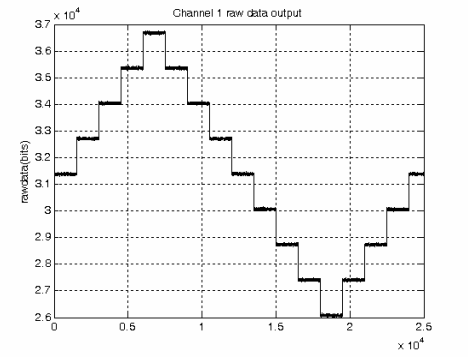

Figure 7- Gyroscope Ch.1 raw output data as response to a stepwise constant turn rate on the rate table

The rotation rate of the rate table is increased in a stepwise manner starting from zero and varying between desired maximum and minimum rates[1] as illustrated in Figure 7. Step size and maximum rate are chosen to be 20º/sec and 80º/sec respectively. Gyroscope data is recorded at each step and the output is compared with the input to obtain the scale factor value as well as to observe any existing nonlinearity. Note that the input-output relationship is linear and there is no hysteresis effect (Figure 8). This indicates that the scale factor is a constant and does not depend on the direction of rotation.

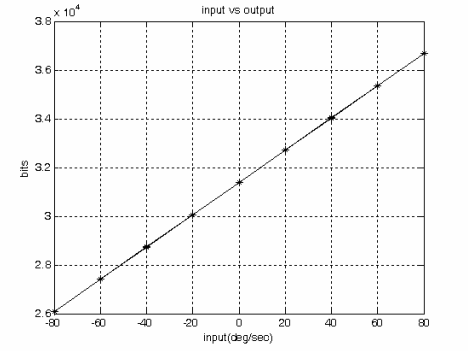

Figure 8 – Gyroscope output raw data values versus input turn-rate. The linear relation is represented by a scale factor.

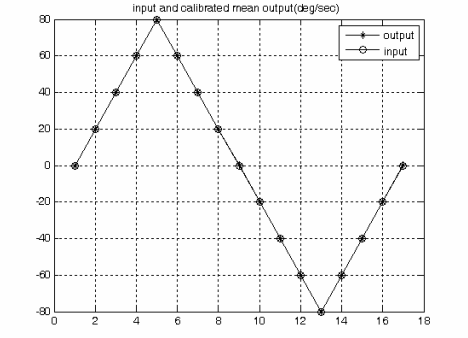

Figure 9- Channel 1 input and calibrated output. Rotation rate varies between +80º/sec and -80º/sec with 20º/sec steps.

After obtaining calibration parameters, raw measurements were converted to physical units. In Figure 9, the plots of input and output rates are given together in units of degrees/second. Note that, the mean value of each noisy data set for each step is used in this figure.

3.3 Impact Tests

Mainly due to their electro-mechanical construction and characteristics, MEMS sensors measurement accuracy is sensitive to sudden movements (impacts) and vibrations. For the gyroscope case, contrary to optical gyroscopes, it is expected that the movement on one axis affects the other axes despite orthogonalization; hence exhibiting a hard to model coupling between the axes. During regular operation, any coupling between the axes can be modelled mathematically and represented using orthogonality matrices $\mathbf{M_A}$ and $\mathbf{M_G}$ and gyro g-dependent bias matrix $\mathbf{B_g}$. However, impacts effect the instrument electro-mechanical operation in complex ways and may be difficult if not impossible to model. To observe the effects of impacts and to obtain a reasonable initial performance estimate of the sensor under impact conditions, a simple experiment has been carried out.

The 3DM-GX1 IMU is placed horizontally on a table with its z-axis pointing in the direction of gravity. An impact is applied along the direction of this axis every second for one minute making sure that other axes do not experience any motion. The effects of impacts are observed on every axis even though there is no applied acceleration on those axes (Figure 10). As expected, we observed that the gyroscopes are also effected (Figure 11).

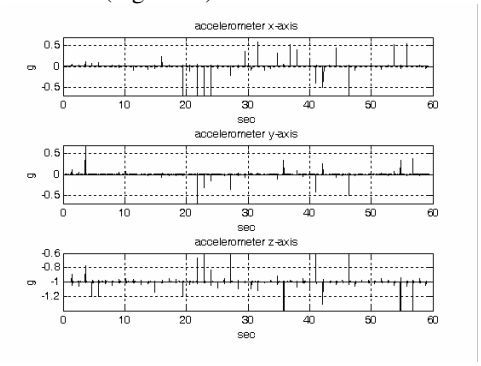

Figure 10- Impacts are applied on z-axis. The effects on other axes are easily observed.

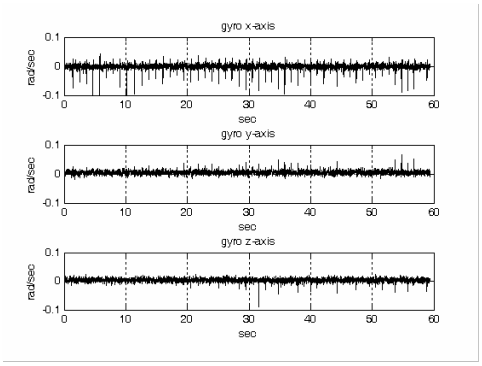

Figure 11- Impacts on z-axis also affect gyroscopes even though there is no angular motion.

3.4 Dynamical Tests

Velocity and position information calculated by integrating inertial measurements suffer from accumulating sensor errors. In order to observe this fact with gyroscope outputs, a rotation test has been conducted. The sensor was placed on the rate table and the table was rotated about the z-axis by 30º steps. Data is recorded continuously throughout the experiment. A plot of the dictated and measured z-axis angular rate is given in Figure 12.

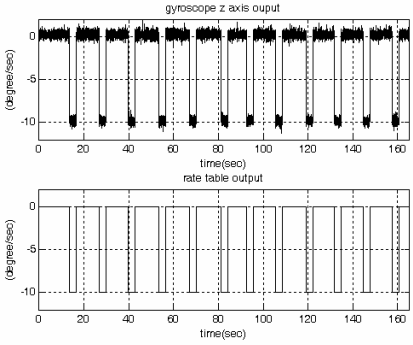

Figure 12- Gyroscope turn rate versus time. Sensor z-axis output and rate table reference input

Angular position is obtained by integrating noisy angular rate sensor output. It is clear from Figure 13 that there is an accumulating (unbounded) error between the calculated and actual angular positions. This is typical behaviour of navigation output variables from inertial sensors.

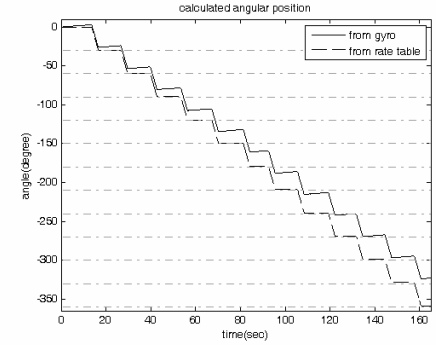

Figure 13- Angular position is calculated from z-axis gyroscope data (blue) and from rate table reference data. Note the increasing error in time.

In view of this behaviour, inertial sensors are usually externally aided by other types of sensors such as magnetometers, cameras and GPS which supply absolute rather than relative measurements. Proper combination of the IMUs generating relative measurements and those sensors generating absolute measurements is an active area of research.

4. CONCLUSION

In this paper, the general characteristics of inertial sensors, namely accelerometers and gyroscopes are explained and their common error models are described. We then focus on MicroStrain 3DM-DX1 MEMS IMU. This sensor is subjected to several of these tests to observe and analyse its error characteristics and calibration parameters. Explanation of basic calibration experiments are given accompanied by their results. Additionally, results of dynamical tests to demonstrate the unbounded errors of angular position calculated from gyroscope data are included. MEMS technology has reached a good performance level in accelerometers. However, gyroscopes still lack in performance as compared to optical technology. They are effected from common phenomena such as linear vibration and impacts that may be present in particular for ground applications. They also require external aids such as magnetometers (which are unfortunately themselves prone to disturbances from electrical and metal surroundings). Our ongoing studies focus on the integration of a camera with a MEMS IMU to generate a bounded error body state estimates of a mobile vehicle.

5. REFERENCES

[1] D.H. Titterton and J.L. Weston , *Strapdown Inertial Navigation Technology*, Peter Peregrinus Ltd. UK

[2] M. Park, "Error Analysis and Stochastic Modeling of MEMS based Inertial Sensors for Land Vehicle Navigation Applications", Ms. Thesis, University of Calgary, April 2004

[3]M.S. Grewall, L.R. Weill, A.P. Andrews, *Global Positioning Systems,Inertial Navigation and Integration*, Wiley&Sons, 2007

[4] http://www.allanstime.com/AllanVariance/index.html

[5] W, Stockwell , "Bias Stability Measurement: Allan Variance", Crossbow Technology, Inc. http://www.xbow.com

[6] T. Sönmez , G. Aslan , "Development of a Software Testbed for Integrated Navigation Systems (In Turkish)", IEEE 15th Signal Processing and Communications Applications, SIU2007, Eskişehir, Turkey

[7] N. Boasman, D. Clarke, S. Davison, R. Stokes, "Advanced Tests Methods for Integrated Navigation Systems", Royal Institute of Navigation, 2005

[8] http://www.imar-navigation.de/englishside/imar.htm

[9] http://www.microstrain.com/3dm-gx1.aspx